

# Acoustic emission during tensile deformation of pre-strained nuclear grade AISI type 304 stainless steel in the unnotched and notched conditions

Chandan Kumar Mukhopadhyay ·  
Tamanna Jayakumar · Baldev Raj ·  
Kalyan Kumar Ray

Received: 18 July 2005 / Accepted: 31 January 2006 / Published online: 29 March 2007  
© Springer Science+Business Media, LLC 2007

**Abstract** Acoustic emission (AE) generated during tensile deformation of notched specimens with varying notch lengths has been compared with those from unnotched specimens of a nuclear grade AISI type 304 stainless steel in the 5 and 30% pre-strained conditions. The results indicate that (a) nature of AE generation is different for different stages of deformation and (b) amount of cold work or pre-strain influences the magnitude of such AE generation. The observed results have been explained using the phenomena of varied localized deformation at the notch tip and deformation-induced  $\alpha'$ -martensite formation in cold worked AISI type 304 stainless steel. An examination of the correlation between total AE counts ( $N$ ) and stress intensity factor ( $K$ ) has shown that the value of the exponent ( $m$ ) in the relationship  $N = AK^m$  decreases with increasing pre-strain. The formation of  $\alpha'$ -martensite in unnotched specimens has been confirmed by equivalent  $\delta$ -ferrite (%) content measurements. The examination of fracture surfaces by scanning electron microscopy (SEM) has indicated that the localized plastic deformation at the notch tip depends on the level of pre-strain.

## Introduction

Acoustic emission technique (AET) is widely used to characterise the deformation and fracture processes in materials. Defects such as dents, notches and cracks present in a structural material influence the acoustic emission (AE) generated from the material under load [1–4]. This is attributed to the fact that defects which act as stress concentrators alter the uniaxial stress field to a multiaxial type during loading and cause localized plastic deformation at nominal stress levels below the yield stress of the net section. The extent of localised plastic deformation depends on the notch depth, size and geometry of the specimen/component, plasticity at the notch tip and the magnitude of the applied stress.

Earlier attempts to study AE generated during tensile deformation of flawed/notched specimens and to compare these with AE signals of unnotched specimens of the same material are a few in number. Comparative analysis of such signals made in beryllium and aluminium alloys [1, 2] and AISI type 304 stainless steel [3, 4] depicts that in materials with secondary phases and inclusions, higher AE is generated in unflawed specimens (higher volume of deforming material) than in flawed specimens (reduced volume of deforming material), opposite to that observed in materials free of second phases like nuclear grade AISI type 304 stainless steel. The higher AE in unflawed specimens than in flawed specimens of materials with secondary phases could be understood by the fact that in such materials in addition to the AE generated by dislocations, AE is also generated by decohesion and/fracture of the second phase particles and the occurrence of such events is more in a large volume of plastically deforming material (in case of unflawed specimens) than that in a lower volume (in case of flawed specimens). This is in agreement with the

---

C. K. Mukhopadhyay (✉) · T. Jayakumar ·  
B. Raj  
Indira Gandhi Centre for Atomic Research, Kalpakkam  
603 102, India  
e-mail: ckm@igcar.ernet.in

K. K. Ray  
Department of Metallurgical & Materials Engineering, Indian  
Institute of Technology, Kharagpur 721 302, India

observation that AE generated during deformation of precipitated alloys is proportional to the volume of the material undergoing plastic deformation [5]. Whereas in a nuclear grade material where AE is mainly associated with dislocation activity, higher AE generated in notched specimens than in unnotched specimens was attributed to the localised deformation at the notch tip [3, 4]. Higher effective strain rate operative at the notch tip also contributed to the increased AE in the notched specimens [6]. It was also observed that increased notch length increases AE generation due to increased localised deformation at the notch tip [4]. Similar result was also reported for a C–Mn pressure vessel steel where increased stress wave energy release (SWER) with increasing notch length before general yielding was attributed to the increased localized plastic deformation at the notch tip [7].

The generation of acoustic activity during tensile deformation of cold worked or pre-strained materials as compared to solution annealed materials is reduced because of reduced glide distance for moving dislocations and the reduced rate of formation of dislocation avalanche [8]. Pre-strained materials also possess reduced plasticity because of higher dislocation density associated with the pre-strained conditions. Palmer [9] reported that AE generated from cold worked specimens with flaws is reduced because of reduced plasticity at the notch tip. It was also reported that both yielding and crack growth in cold worked specimens are very quiet [9]. But no comparative study of AE between the two types of specimens (unflawed and flawed) mentioned above, in the case of pre-strained materials is available in the literature. The major aim of the present investigation is to generate and examine such results.

AISI type 304 stainless steel is known to undergo deformation-induced transformation from austenite to  $\alpha'$ -martensite at ambient temperature [10]. The phenomenon of deformation-induced martensitic transformation in metastable stainless steels has been classified as two types viz. strain-induced and stress-assisted [11]. While the strain-induced transformation occurs by creation of new sites and embryos by plastic deformation of the parent austenite, the latter takes place under the application of elastic stress and involves the same sites and embryos existing in the matrix [11]. It is known from an earlier investigation that in AISI type 304 stainless steel, deformation-induced transformation from austenite to martensite produces detectable acoustic activity [12]. The magnitude of AE generation from such transformation is dependent on the amount of prior cold work (PCW); being higher for lower amount of PCW ( $\leq 10\%$ ) and lower for PCW  $\geq 20\%$ . This could be understood by the fact that small amount of PCW stimulates while higher amount of PCW retards martensite formation during subsequent

deformation [13, 14]. Thus, the present study is also aimed to analyse whether the nature of such AE generation prevailing in unnotched specimens of cold worked AISI type 304 stainless steel also occurs in notched specimens.

In an earlier investigation [1], total AE counts ( $N$ ) and stress intensity factor ( $K$ ) were correlated as

$$N = AK^m \quad (1)$$

where  $A$  and  $m$  are constants. The value of  $m$  was theoretically predicted as 4 [1] whereas experimental results on different materials like C–Mn steel [7, 9, 15], A533 Grade B steel [16] and aluminium alloys [1, 17] showed the value to lie in a wide range. The reported lower values of the exponent (1–6) in the  $N$ – $K$  relationship were attributed to the plastic zone formation at the notch tip while the higher values of  $m$  ( $>8$ ) were assigned to the phenomenon of crack growth [17]. In nuclear grade 304 stainless steel, the value of  $m$  has been found to lie between 1.1 and 1.9 in the solution annealed condition and this has been attributed to the localized deformation at the notch tip [4]. But in none of the earlier investigations, the effect of prior cold work on the value of  $m$  was studied. Another aim of this study is thus to examine such correlation for notched specimens of pre-strained nuclear grade AISI type 304 stainless steel.

## Experimental

The chemical composition of the AISI type 304 stainless steel used in this study is shown in Table 1. The steel was obtained in the solution annealed condition (1,323 K for 1 h, WQ). Inclusion analysis in the polished samples indicated the size of the inclusions to be in the range of 0.5–1  $\mu\text{m}$  and their numbers are very few. The microstructure of the steel in the solution annealed condition is austenite and the average grain size is  $55 \pm 3 \mu\text{m}$ .

Flat tensile specimens having gauge dimensions  $36 \times 8 \times 5 \text{ mm}$  were fabricated from the solution annealed plate of this steel. All the specimens were polished with 400 grit emery papers to obtain a uniform surface finish. The pre-strained specimens were made by deforming the solution annealed specimens up to 5 and 30% nominal strain levels in an Instron 1195 Tensile Testing Machine (M/s. Instron, UK) and then by remarking the gauge lengths. In the solution annealed and pre-strained specimens, notches with  $a/W$  ratios ( $a$  = notch length and

**Table 1** Chemical composition (wt%) of AISI type 304 stainless steel

Elements	C	Cr	Ni	Mn	Si	S	P	Fe
Wt%	0.08	18.0	10.5	2.0	1.0	0.002	0.03	Bal.

$W$  = gauge width of the tensile specimen) in the range of 0.1–0.25 were made at the centre of the gauge length by spark erosion machining. Figure 1a shows the details of the tensile specimens in the as-annealed condition prior to introducing the pre-strain and Fig. 1b shows the details of the notch made in different specimens. It should be noted that pre-straining to 5 and 30% increases the gauge length and decreases the gauge width and thickness of the specimens. The  $a/W$  ratios of the notches in the pre-strained specimens were maintained in the range of 0.1–0.25 by taking into account the decrease in the gauge width with increasing pre-straining. The notch length and the notch tip radius were measured using a Measurescope MM2 (M/s. Nikon, Japan) having a resolution of 1 micron. The included angle of the notches and the radius at the notch tip were maintained within  $60 \pm 1^\circ$  and  $0.2 \pm 0.05$  mm, respectively. This was done by changing the notch dimensions for the notches of the specimens with different pre-straining. Tensile tests of all the specimens were carried out at a cross head speed of  $1.67 \times 10^{-3}$  mm/s at ambient temperature (300 K).

Figure 2 shows the schematic of the experimental set up used to record the AE signals generated during tensile tests of the pre-strained specimens. Acoustic emission signals were recorded and analysed using a Spartan 2000 acoustic emission system (M/s. Physical Acoustic Corporation, USA). A piezoelectric transducer having a resonant frequency at 175 kHz, a preamplifier (40 dB gain) and a compatible filter (100–300 kHz) were used to capture the AE signals. The transducer used was of 8 mm diameter and

10 mm height. The transducer was fixed at the gauge to shoulder transition region of different specimens using silicon grease as couplant. For recording AE signals during deformation, proper location of the transducer is important in order to record the AE signals with high sensitivity. The AE signal generated during deformation of a material is significantly influenced by the resonance and transmission characteristics of both the specimen (geometry as well as acoustic properties) and the transducer. In practice, this is governed by background noise and attenuation of the acoustic waves that restrict the useful detection range. The position of the transducer is chosen to keep the transducer close to the primary sources of acoustic emission generation. This requirement is met by mounting the transducer at the gauge to shoulder transition region of the tensile specimen which is outside the gauge length of the specimen and experiences less deformation than the gauge region. Thus the problem of slipping the transducer during the testing is minimized. At the same time this also allows a larger area of the gripped region so that the specimen is gripped properly to the testing machine.

A total gain of 88 dB and a threshold of 38 dB were so selected that no external noise was recorded during the experiments. This was verified by repeatedly loading and unloading a dummy specimen to more than 1.5 times the maximum load expected to be taken by any of the speci-

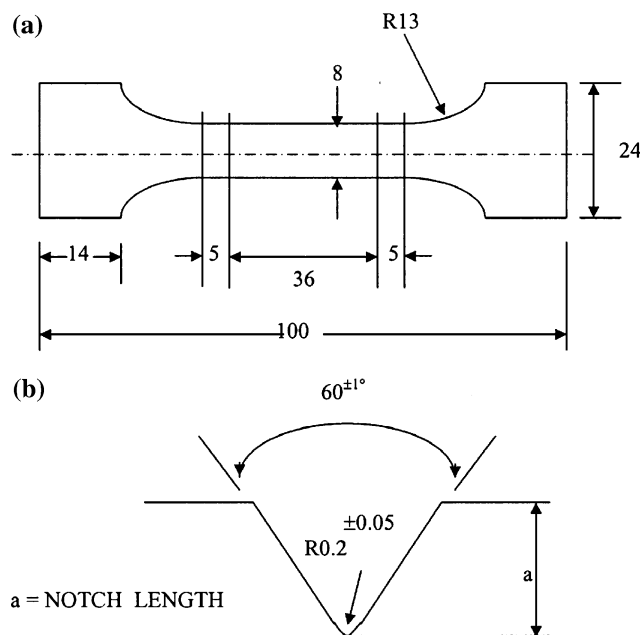


**Fig. 1** Details of (a) tensile specimens prior to introducing pre-strain and (b) notch

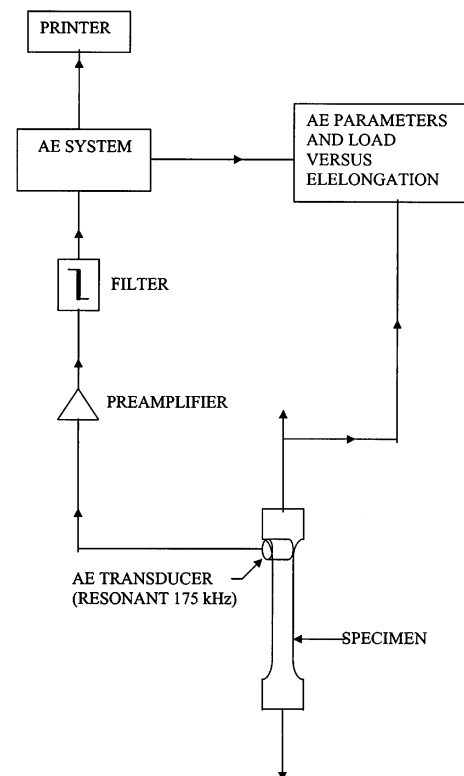


**Fig. 2** Schematic of experimental setup

mens used in the present study. After the first cycle of loading, no emission was generated during the subsequent cycles. This indicated that the AE signals were not recorded either from the machine or from external noise. AE counts recorded during the tests were used for analysing the results.

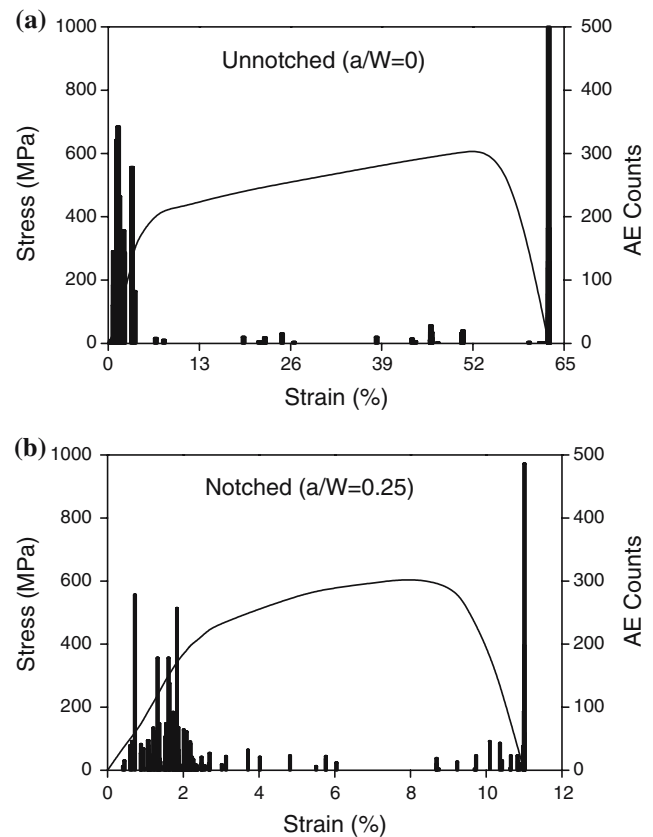
## Results

Figure 3a, b show the variations in stress and AE counts with strain for typical unnotched and notched ( $a/W = 0.25$ ) specimens in the 5% pre-strained condition. Similarly the variations between stress and AE counts with strain for such specimens in the 30% pre-strained condition are shown in Fig. 4a, b. The stress and strain values plotted in Figs. 3, 4 are engineering stress strain values. It can be seen from Figs. 3, 4 that significant AE is generated in the region before or near the macroscopic yielding for all the specimens. In addition to this, AE is also observed in the post-yield regime. It can be also seen that AE generated in different regimes of the stress–strain curve is not uniform and depends on the regime of deformation and level of pre-strain. In order to understand the AE generated in different specimens more distinctly, AE counts obtained up to (i) macroyielding i.e. up to 0.2% offset yield strength (YS), (ii) up to ultimate tensile strength (UTS) and (iii) for complete tensile test (except instantaneous final fracture) of different specimens have been determined. Figure 5 shows the total AE counts obtained for (a) up to macroyielding ( $N_y$ ), (b) up to UTS ( $N_{uts}$ ) and (c) for complete tensile test ( $N_t$ ) vs.  $a/W$  for the 5% pre-strained and 30% pre-strained conditions.

In order to further comprehend the AE counts generated between the two types of specimens (unnotched and notched) and for the two pre-strained (5 and 30%) conditions, the difference in counts between these two types of specimens was computed. The normalised difference in total AE counts ( $\Delta N$ ) between notched and unnotched specimens for the three deformation regimes mentioned above was determined as follows:

$$\Delta N = (N_{ns} - N_{us})/N_{us} \quad (2)$$

where  $N_{ns}$  and  $N_{us}$  are the average total counts generated for the notched and unnotched specimens, respectively, for any given regime. The average values were taken from at least two measurements. The values of  $\Delta N$  thus obtained were designated as  $\Delta N_y$ ,  $\Delta N_{uts}$  and  $\Delta N_t$  for the regimes (i) up to macroyielding, (ii) up to UTS and (iii) for complete tensile test, respectively. The variation of  $\Delta N_y$  with  $a/W$  for the 5 and 30% pre-strained conditions is shown in Fig. 6a. Similarly the variations for  $\Delta N_{uts}$  and  $\Delta N_t$  with  $a/W$  for the



**Fig. 3** Variation in nominal stress and AE counts with nominal strain for (a) unnotched and (b) notched specimens of 5% pre-strained 304 stainless steel

above two conditions are shown in Fig. 6b, c, respectively. The increase in the value of  $\Delta N$  with  $a/W$  shown in Fig. 6 indicates higher AE activity in notched specimens as compared to unnotched specimens.

The results in Figs. 3–6 indicate several inferences: (i) irrespective of the level of pre-strain and type of specimen, AE generated in the post-yield regime is drastically reduced as compared to that in the regime prior to and during macroyielding (Figs. 3, 4), (ii) for any type of specimen, AE generated is higher for 5% pre-strain as compared to 30% pre-strain (Figs. 3–5), (iii) total counts generated for all the regimes i.e. up to macroyielding, up to UTS and for complete tensile test, in general, are higher for notched specimens than unnotched specimens (Fig. 5). The values of total counts appear to be bounded by similar scatter bands in all the notched specimens irrespective of the variation in the notch length, (iv) for any regime, the parameters  $\Delta N_y$ ,  $\Delta N_{uts}$  and  $\Delta N_t$  possess higher values for notched specimens than unnotched ones but do not change significantly with  $a/W$ . These parameters appear to be better described by a constant ( $c$ ) multiplication of the total count values of unnotched specimens. The values of  $c$  were determined from Fig. 6a–c and are also shown in the same

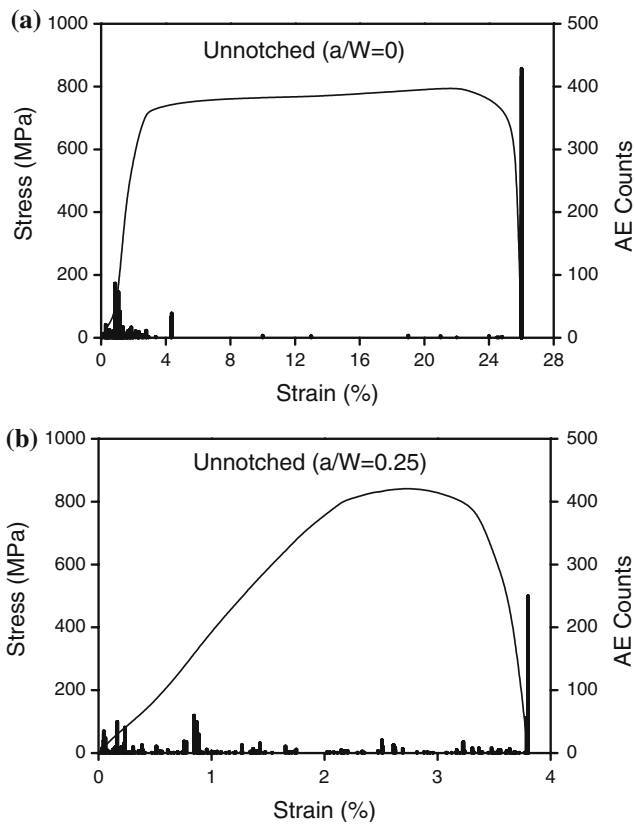


**Fig. 4** Variation in nominal stress and AE counts with nominal strain for (a) unnotched and (b) notched specimens of 30% pre-strained 304 stainless steel

figures. This indicates that the value of  $c$  decreases with increasing pre-strain, and for any pre-strain,  $c$  decreases for counts generated up to UTS but increases again for counts generated for the complete tensile test.

The total AE counts ( $N$ ) obtained for notched specimens of two pre-strained conditions have been examined with respect to the stress intensity factor ( $K$ ) corresponding to the yield load. The magnitude of the stress intensity factor ( $K$ ) was calculated using the following equation for single edge notched tensile specimen [18]:

$$K = (P/WB)a^{1/2}[1.99 - 0.41(a/W) + 18.7(a/W)^2 - 38.48(a/W)^3 + 53.85(a/W)^4] \quad (3)$$

where,  $K$  is in  $\text{Mpa m}^{1/2}$ ;  $P$ , load (kg);  $B$ , specimen thickness (mm);  $W$ , specimen width (mm) and  $a$ , notch length (mm).

The variation of  $N$  with  $K$  for a notched specimen in a log-log scale indeed shows linear relation [4]. The slope of such linear plots represents the value of the exponent  $m$  in Eq. 1 and such  $m$  values for different notched specimens of 5 and 30% pre-strained conditions were estimated. The values of  $m$  for different  $a/W$  ratios and

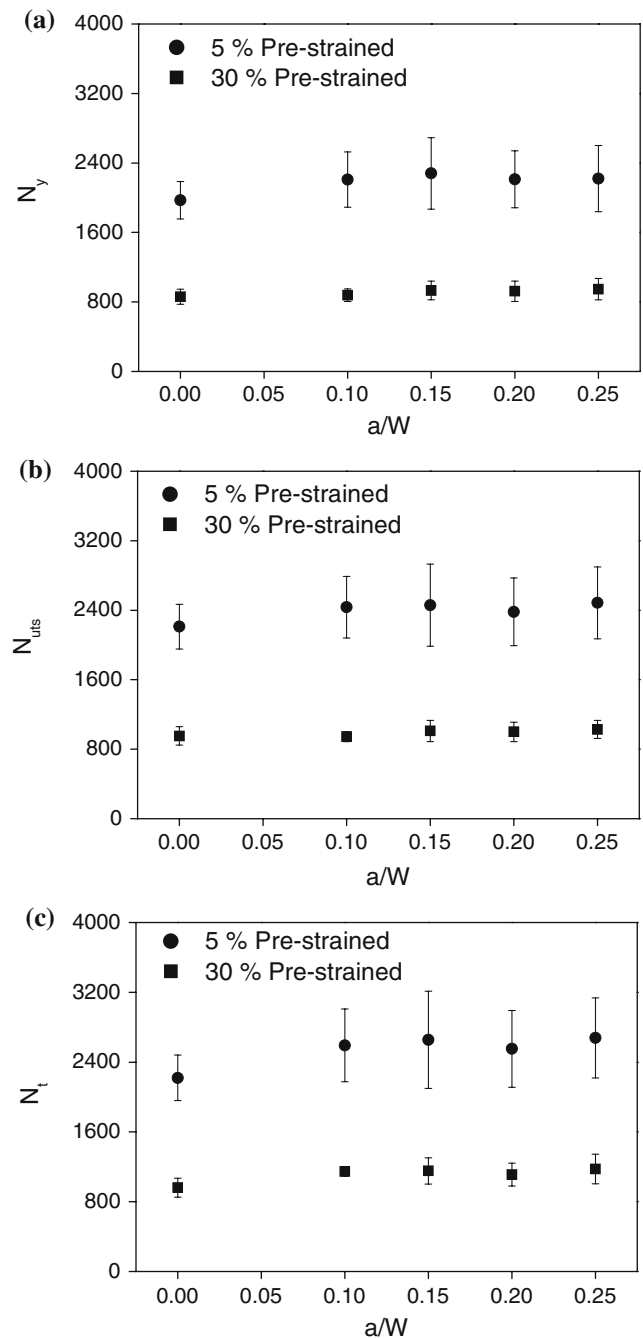


**Fig. 5** Variation in total AE counts for (a) up to macroyielding ( $N_y$ ), (b) up to ultimate tensile strength ( $N_{uts}$ ) and (c) for complete tensile test ( $N_t$ ) with  $a/W$  for 5 and 30% pre-strained 304 stainless steel

for the different conditions, corresponding values of stress intensity factor over which the  $m$  values are estimated and the correlation coefficients of the best fit between  $N$  and  $K$  are given in Table 2. It can be seen from Table 2 that, (i) there exists a good correlation between  $N$  and  $K$ , (ii) the magnitude of  $m$  for all the notched specimens lies below the theoretically predicted value of 4 for fatigue pre-cracked specimens reported in the lit-

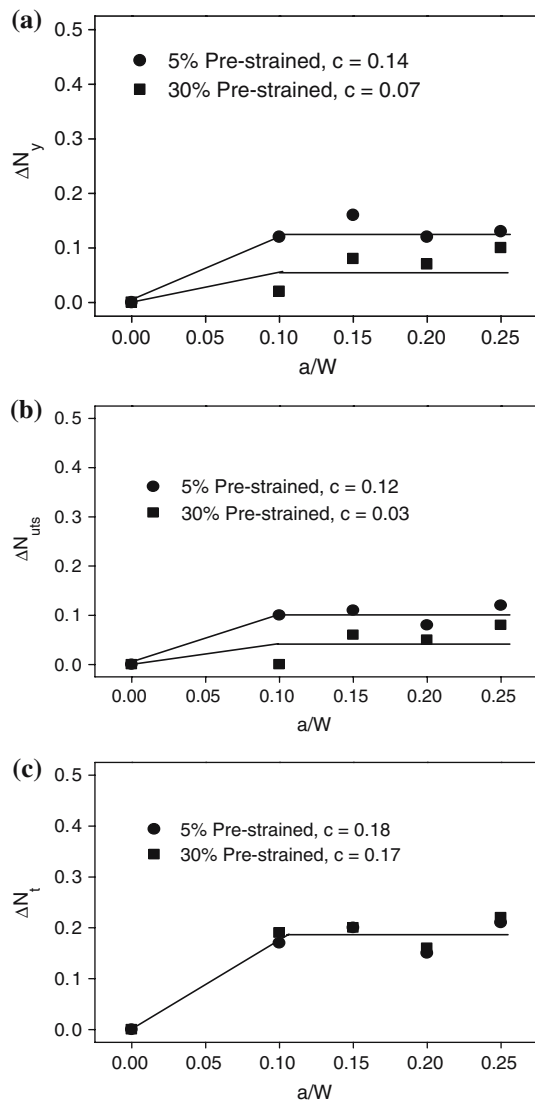


**Fig. 6** Variation in normalized difference in total counts between notched and unnotched specimens for (a) up to macroyielding ( $\Delta N_y$ ), (b) up to ultimate tensile strength ( $\Delta N_{ults}$ ) and (c) for complete tensile test ( $\Delta N_t$ ) with  $a/W$

erature [1] and (ii) the values of  $m$  for 5% pre-strained specimens is marginally higher (1.1–1.5) than that for 30% pre-strained specimens (1.2–1.3).

**Table 2** Values of the exponent ( $m$ ) in the Eq.  $N = AK^m$ , corresponding values of stress intensity factor ( $K$ ) at macroyielding and correlation coefficients of the best fit for different notched specimens

$a/W$	Pre-strain (%)					
	5			30		
	Ranges in $K$	$m$	Correlation coefficient	Ranges in $K$	$m$	Correlation coefficient
0.10	1.5–21.2	1.10	0.92	3.8–42.2	1.19	0.97
0.15	2.2–32.4	1.12	0.95	5.6–59.0	1.24	0.90
0.20	3.7–36.7	1.23	0.95	5.7–70.6	1.26	0.97
0.25	6.9–46.0	1.48	0.90	5.9–88.6	1.22	0.96

## Discussion

The results obtained during tensile deformation of different specimens would be discussed in this section with respect to the (i) generation of AE activity in cold worked AISI type 304 stainless steel, (ii) effect of notch on AE and (iii) relation between  $N$  and  $K$ .

### Generation of AE activity

Acoustic emission during tensile deformation of nuclear grade austenitic stainless steel is mainly generated by dislocation activity [19]. AE during tensile deformation of pre-strained nuclear grade AISI type 304 stainless steel occurs from generation and motion of dislocations and deformation-induced martensitic transformation. The generation of AE due to dislocation activity is reduced in the cold worked condition as compared to the annealed condition. On the other hand, the nature of deformation-induced  $\alpha'$ -martensite formation changes from strain-induced type in the annealed condition to both stress-assisted (assisted by elastic stress in the lower strain levels) and strain-induced (during post-yield deformation) types in the pre-strained condition. In the earlier investigation [12], significant AE generated during post-yield deformation of the annealed specimens was attributed to the strain-induced martensitic transformation, as a minimum amount of strain is necessary for commencement of this transformation. But in cold worked specimens, significant AE was observed at lower strain level up to macroyielding than that beyond yielding and this was attributed to the higher amount of martensite formed in the lower strain levels [12]. In the case of present investigation, it can be seen that AE generated at lower strain level is significantly higher than that at higher strain level irrespective of the type of specimen and level of pre-strain. This is attributed to the occurrence of stress-assisted martensite formation at lower strain level in the pre-strained specimens. Comparison of Figs. 3–5 also indicates that higher AE is generated in the 5% pre-strained (PS) condition compared to 30% PS condition. This is

attributed to the formation of higher amount of stress-assisted  $\alpha'$ -martensite in the 5% PS condition as compared to the 30% PS condition. Activation of the transformation by lower amount of prior cold work and retardation of the transformation by higher amount of prior cold work is reported in the literature [13, 14]. But in the notched specimens, in addition to the stress-assisted martensite, strain-induced martensite also forms by the localized plastic deformation of the material surrounding the notch tip, being higher for 5% than 30% pre-strain. The higher AE generation in the 5% pre-strained specimens compared to 30% pre-strained specimens is attributed to this also. The occurrence of localized plastic deformation at the notch tip during tensile deformation of AISI type 304 stainless steel has been shown in an earlier paper [20].

The formation of  $\alpha'$ -martensite during tensile deformation has been confirmed by estimating equivalent  $\delta$ -ferrite (%) content in various unnotched specimens using Ferritoscope FE-8. The measurements were done on both sides of the tensile specimens in the direction parallel to the tensile axis and the average values were taken. The sensitivity of measurements of Ferritoscope FE-8 was as follows: 0.1% in the smallest scale (0–3% equivalent  $\delta$ -ferrite), 0.2% in the medium scale (0–10% equivalent  $\delta$ -ferrite) and 0.5% in the highest scale (0–30% equivalent  $\delta$ -ferrite). The results obtained are plotted in Fig. 7 as the variation in equivalent  $\delta$ -ferrite (%) content with distance from the fracture surface for (a) as pre-strained, (b) pre-strained and tensile tested and (c) difference between pre-strained and tensile tested and as pre-strained conditions. Figure 7 indicates that pre-straining up to 30% only induces martensite as compared to annealed and 5% PS conditions (Fig. 7a). After tensile testing, martensite is maximum in the 30% PS specimens as compared to annealed and 5% PS specimens (Fig. 7b). The difference in martensite between pre-strained and tensile tested and as pre-strained conditions (Fig. 7c) is higher for annealed and 5% PS as compared to 30% PS specimens. This indicates the formation of higher amount of martensite during tensile testing in the 5% PS compared to 30% PS specimens. Higher amount of the equivalent  $\delta$ -ferrite (%) content near the point of fracture and its decrease with increasing distance from the fracture region can be understood by higher strain at the fracture region which causes higher amount of transformation. It should be noted that the equivalent  $\delta$ -ferrite (%) measurement by a Ferritoscope is influenced by prior cold work, anisotropy and/or surface condition of the material. In the present investigation, equivalent  $\delta$ -ferrite (%) content measurements were done on the specimens with different amount of prior cold work and hence the values depicted in Fig. 7 can be considered as relative values instead of absolute values.

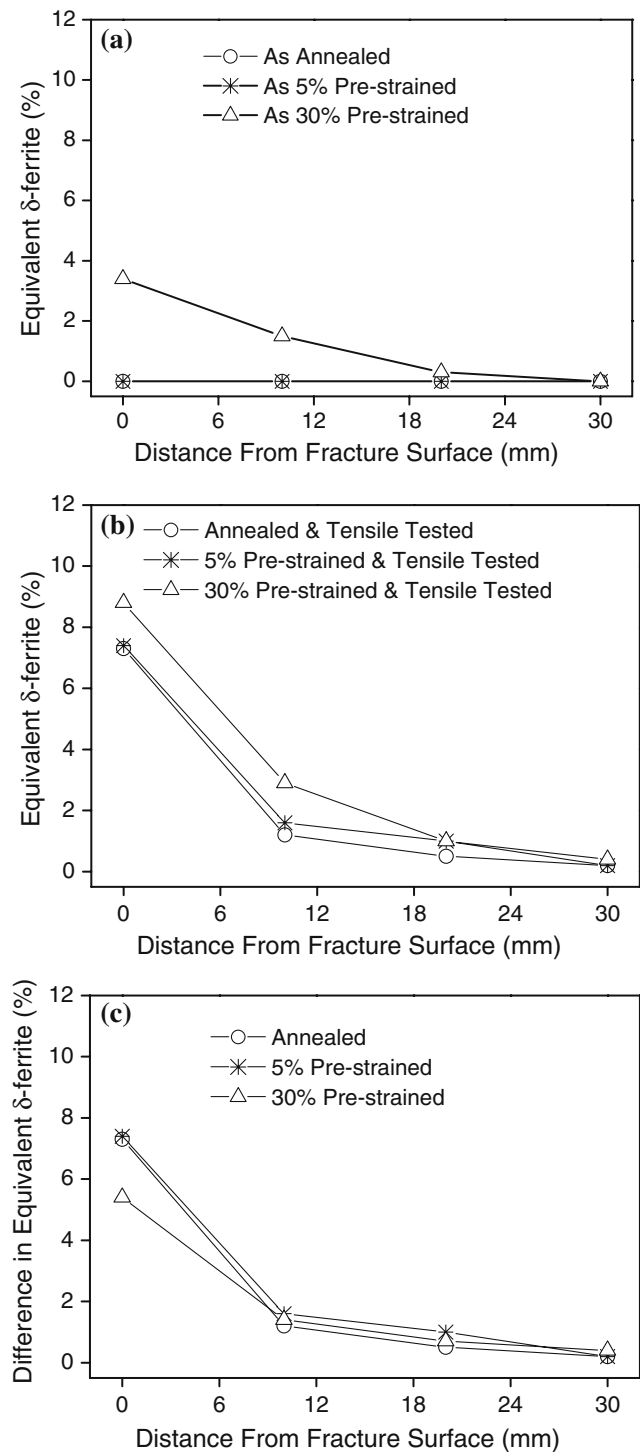


**Fig. 7** Variation in equivalent  $\delta$ -ferrite (%) content with distance from the fracture surface for (a) as pre-strained, (b) pre-strained and tensile tested and (c) difference between pre-strained and tensile tested and as pre-strained conditions

#### Effect of notch on AE

The difference in acoustic activity between the two types of specimens (unnotched and notched) and for the two dif-

ferent conditions (5% pre-strained and 30% pre-strained) can be considered to arise due to difference in the dislocation activity. In materials with presence of second phases like beryllium and aluminium alloys and commercial grade AISI type 304 stainless steel, the major source of AE is the decohesion and/or fracture of second phase particles and this generates burst type AE signals. The higher AE generated in unflawed specimens than in flawed specimens of such materials could be explained by the fact that decohesion and/fracture events predominate in generating AE signals than the other sources since the probability of occurrence of such decohesion is more in unflawed specimens (higher volume of deforming material) than in flawed specimens (reduced volume of deforming material) [1–3]. In comparison to such materials, in nuclear grade materials, the generation and motion of dislocations mainly generate AE. The higher AE generated up to macroyielding in the notched specimens than unnotched specimens of nuclear grade AISI type 304 stainless steel in the present investigation can thus be attributed to the phenomenon of localized deformation at the notch tip, in agreement with the earlier studies [3, 4]. Higher AE in the notched specimens can be also attributed to the higher effective strain rate at the notch tip [6].

The AE counts generated in the notched specimens do not increase appreciably with increase in notch length and also appear to be bounded by similar scatter bands for all the notched specimens. Increased AE generation during tensile deformation of annealed AISI type 304 stainless steel with increasing notch length reported earlier was attributed to the increased localised deformation around notch tip [3]. Investigations conducted on C–Mn steel [7] showed that the stress wave energy release (SWER) during tensile deformation of notched specimens is proportional to the size of the plastic zone before general yielding. On the other hand, in pre-strained materials, the generation of acoustic emission during tensile deformation is known to get lowered because of the reduced glide distance for moving dislocations and the reduced rate of formation of dislocations [8]. Pre-strained materials possess increased strength with an accompanied decrease in ductility and this, in turn, reduces the magnitude of the localized plastic deformation around notches. With increasing notch length in pre-strained specimens, the extent of such localized deformation depends on the degree of prior cold work, being maximum for the solution annealed condition and reduces with increasing pre-strain. This can be understood by comparing notch strengthening for different pre-strains. The magnitude of notch strength ratio (NSR) at yield was determined as the ratio of the yield strength of notched specimen to the yield strength of unnotched specimen and plotted as a function of  $a/W$  for different pre-strains (Fig. 8). The results of solution an-

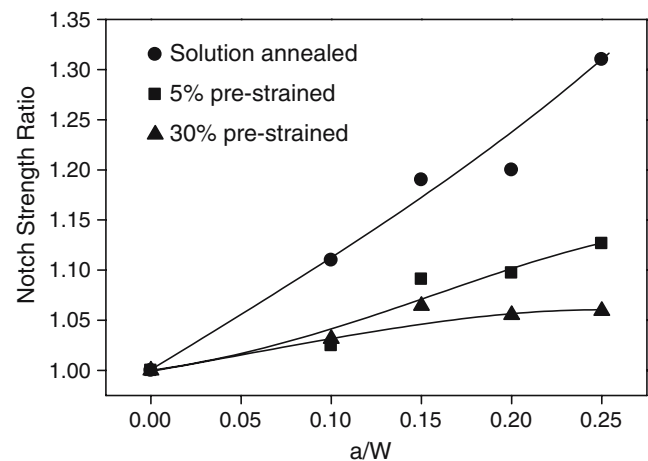


Fig. 8 Variation of notch strength ratio at yield with  $a/W$

nealed specimens are also included in this plot for comparison. These results unambiguously indicate the occurrence of notch strengthening in this material and the notch strengthening decreases with increasing pre-strain. The presence of a notch in a tensile specimen results in stress triaxiality. The effect of notch on tensile properties is governed by the amount of stress triaxiality produced by the notch and the ability of a material to accommodate deformation due to stress concentration. Consequently, the yield strength of a notched specimen is greater than the yield strength of an unnotched specimen of ductile materials. The phenomenon of notch strengthening in ductile material has been reported [21]. The reduced dislocation activity around notch tip for the higher pre-strain (30%) as compared to the lower pre-strain (5%) is thus also considered to give rise to the reduced AE counts ( $N_y$ ,  $N_{uts}$  and  $N_t$ ) in 30% pre-strained specimens than in 5% pre-strained ones. This also leads to the characteristic variation of  $\Delta N_y$  and  $\Delta N_{uts}$  with  $a/W$  as shown in Fig. 6a, b and results in reduction in the value of the constant  $c$  with increasing pre-strain. These results are in agreement with the reported observation of Palmer on C–Mn steel that yielding in 10–20% pre-strained materials are quiet and a pre-strain of 10% is adequate to remove most of the emissions arising from plastic yielding at the crack tip [9]. The value of  $c$  is reduced for  $\Delta N_{uts}$  and increased again for  $\Delta N_t$  as compared to that for  $\Delta N_y$ . The reduction in the value of  $c$  for  $\Delta N_{uts}$  can be understood by the occurrence of blunting of the notch tip after macroyielding. The increase in the value of  $c$  for  $\Delta N_t$  can be understood by higher AE generated due to tearing in the notched specimens during necking elongation [3, 4].

The fracture surfaces of the notched specimens ( $a/W = 0.25$ ) in the annealed, 5% PS and 30% PS conditions were examined under a scanning electron microscope



(SEM Model 501Q of M/s. Philips). For this, small samples were cut from the fracture regions of the tensile tested specimens. The photomicrographs of the fracture surfaces were taken at a distance of around 50  $\mu\text{m}$  from the notch tip for all the specimens and are shown in Fig. 9a–c for the annealed, 5% pre-strained and 30% pre-strained conditions, respectively. The photomicrograph in the annealed condition (Fig. 9a) indicates ductile dimple type fracture, characteristic of materials possessing higher plasticity at the notch tip. But with increasing pre-strain, size of the dimples is reduced and this indicates reduced plasticity at the notch tip with increasing pre-strain. This observation substantiates the earlier argument that the magnitude of the localized plastic deformation at the notch tip decreases with increasing pre-strain.

#### Relation between $N$ and $K$

The values of the exponent ( $m$ ) in the  $N$ – $K$  relation as depicted in Table 2 indicate that the values of  $m$  are below 4 for both the pre-strained conditions. In an earlier investigation [1], the value of  $m$  was theoretically predicted as 4 assuming that AE generated in a flawed specimen is proportional to the volume of the plastically deforming material ahead of the crack tip. Experiments conducted on aluminium alloys however showed  $m$  to lie between 4 and 8 [1]. In C–Mn steel, the stress wave energy release (SWER) was reported to be linearly proportional to the plastic zone length before general yielding and  $\text{SWER} \propto K^2$  [7]. Lower value of  $m$  ( $=2$ ) was also reported for C–Mn steel and this was explained by the fact that 95% of the AE activity was generated up to a plastic strain of 0.002 [9, 16]. For notched specimens of aluminum alloys, values of  $m$  in the range of 1 and 6 was reported and this was attributed to the plastic zone formation at the crack tip [17]. It was also reported that specimens with machined notches result in lower value of  $m$  ( $=1$ ) as compared to the specimens with fatigue precracks [17]. The observed lower value of  $m$  ( $<4$ ) in the present study is thus attributed to the fact that, in notched specimens of nuclear grade AISI type 304 stainless steel, AE at lower strain is mainly associated with plastic deformation around blunt notches. This is in agreement with the values of  $m$  (1.1–1.9) obtained in this material in the solution annealed condition examined for  $a/W$  ratios between 0.1 and 0.25 [4]. Comparison of the above mentioned values of  $m$  in the annealed condition with the results depicted in Table 2 indicates that the ranges in the values of  $m$  is highest for the solution annealed condition (1.1–1.9) and is lowest for 30% pre-strained specimens; the magnitude of  $m$  for 5% pre-strained specimens is marginally higher (1.1–1.5) than that for 30% pre-strained specimens (1.2–1.3).

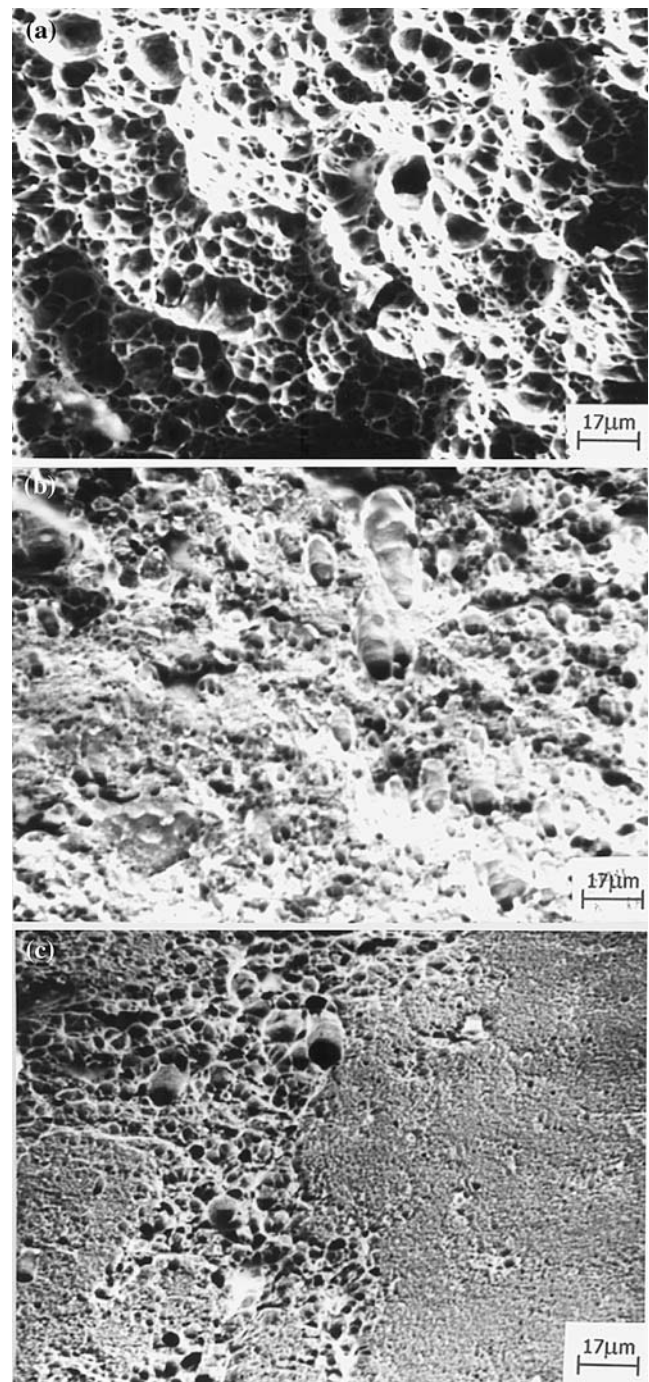


**Fig. 9** SEM photomicrographs of fracture surfaces ahead of the notch tip for (a) annealed, (b) 5% pre-strained and (c) 30% pre-strained conditions

#### Conclusion

Acoustic emission generated during tensile tests of unnotched and notched specimens of pre-strained nuclear grade AISI type 304 stainless steel has shown that acoustic activity is a function of the type of specimen (notched or

unnotched) and magnitude of pre-strain (5 or 30%). The higher AE counts for 5% pre-strained specimens than 30% pre-strained specimens has been explained using stimulation of deformation-induced martensitic transformation in AISI type 304 stainless steel. Acoustic activity for notched specimens has been found to be higher than that for unnotched ones and the difference does not increase significantly with increasing notch length. These aspects are explained by the fact that AE in nuclear grade 304 stainless steel is primarily governed by dislocation activity and prior cold work affects AE generation from such sources. The value of the exponent ( $m$ ) in the correlation  $N = AK^m$  is reduced with increasing pre-strain. Increasing pre-strain reduces localized deformation around notch as evidenced by examination of the fracture surfaces of the notched specimens under SEM.

**Acknowledgments** Authors thank Dr S.L. Mannan, Director, Metallurgy and Materials Group, Indira Gandhi Centre for Atomic Research (IGCAR), Kalpakkam-603 102, India, for useful discussions. Authors also thank Mr P. Kalyanasundaram, Associate Director, Inspection Technology Group, IGCAR, for useful discussions.

## References

- Dunegan HL, Harris DO, Tatro CA (1968) Engg Frac Mech 1:105
- Philips AL, Godinez VG, Stafford SW (1985) Mat Eval 43:420
- Mukhopadhyay CK, Ray KK, Jayakumar T, Raj B (1998) Mater Sci Engg A255:98
- Mukhopadhyay CK, Jayakumar T, Raj B, Ray KK (2000) Mater Sci Engg A276:83
- James DR, Carpenter SH (1976) Scripta Metall 10:779
- Dunegan HL, Green AT (1972) ASTM STP 505. American Society for Testing and Materials, PA, pp 100–113
- Ishikawa K, Kim HC Jr (1974) J Mater Sci 9:737
- Agarwal ABL, Frederick JR, Felbeck DK (1970) Metall Trans 1A:1069
- Palmer IG (1973) Mater Sci Engg 11:227
- Maxwell PC, Goldberg A, Shyne JC (1974) Metall Trans 5A:1305
- Olson GB, Cohen M (1972) J Less Common Metals 28:107
- Mukhopadhyay CK, Kasiviswanathan KV, Jayakumar, Raj B (1993) J Mater Sci 28:145
- Guimaraes JR, Shyne JC (1970) Scripta Metall 4:1019
- Strife JR, Carr MJ, Ansell GS (1977) Metall Trans 8A:1471
- Palmer IG, Heald PT (1973) Mater Sci Engg 11:181
- Ying SP (1975) J App Phys 46:2882
- Kanji Ono, Ucisik J (1976) Mat Eval 34:32
- Hartbower CE, Gerberich WW, Liebowitz H (1968) Engg Frac Mech 1:291
- Raj B, Jayakumar T (1990) in Acoustic emission: current practices and future directions, ASTM STP 1077. American Society for Testing and Materials, Philadelphia, PA, 1990, pp 218–241
- Mukhopadhyay CK, Jayakumar T, Raj B, Ray KK (2002) Mater Sci Tech 18:1133
- Hertzberg RW (1983) Deformation and fracture mechanics of engineering materials. John Wiley & Sons, Inc